[Frontiers in Bioscience 13, 5681-5692, May 1, 2008]

# Self-assembly of amyloid-forming peptides by molecular dynamics simulations

**Guanghong Wei[1], Wei Song[1], Philippe Derreumaux[2], Normand Mousseau [3]**

*[1]National Key Surface Physics Laboratory and Department of Physics, Fudan University, Shanghai 200433, China, [2] Laboratoire de Biochimie Theorique, UPR 9080 CNRS, Institut de Biologie, Physico-Chimique et Universite Paris 7,13 rue Pierre et Marie Curie, 75005 Paris, France, [3] Departement de Physique and Regroupement Quebecois sur les Materiaux de Pointe, Universite de Montreal, C.P. 6128, succursale centre-ville, Montreal (Quebec), Canada*

## TABLE OF CONTENTS



## 1. ABSTRACT

Protein aggregation is associated with many neurodegenerative diseases. Understanding the aggregation mechanisms is a fundamental step in order to design rational drugs interfering with the toxic intermediates. This self-assembly process is however difficult to observe experimentally, which gives simulations an important role in resolving this problem. This study shows how we can proceed to gain knowledge about the first steps of aggregation. We first start by characterizing the free energy surface of the Abeta (16-22) dimer, a well-studied system numerically, using molecular dynamics simulations with OPEP coarse-grained force field. We then turn to the study of the NHVTLSQ peptide in 4-mers and 16-mers, extracting information on the onset of aggregation. In particular, the simulations indicate that the peptides are mostly random coil at room temperature, but can visit diverse amyloid-competent topologies, albeit with a low probability. The fact that the 16-mers constantly move from one structure to another is consistent with the long lag phase measured experimentally, but the rare critical steps leading to the rapid formation of amyloid fibrils still remain to be determined.

## 2. INTRODUCTION

The deposition of amyloid fibrils is a hallmark of more than 20 human diseases including Alzheimer's disease (AD), type-II diabetes, spongiform encephalopathies (SE), and dialysis-related amyloidosis (1-4). All these proteins differ in amino acid composition and length and adopt distinct structures in their monomeric forms. For instance, the beta-Amyloid protein of 40 or 42 residues, associated with AD, is random coil in solution (5), while the 210-residue prion protein, associated with transmissible spongiform encephalopathies (TSE), is mainly composed of a random-coil N-terminal domain and an essentially alpha-helical C-terminal domain (6). However, all these proteins aggregate into amyloid fibrils sharing a common cross beta-sheet structure with beta-strands perpendicular to the fibre axis and beta-sheets propagating along the direction of the fibril (7, 8).

There is recent experimental evidence suggesting that the toxicity may be caused by the oligomers formed in the early stage of fibril formation, independently of the protein length (4, 9-11). It is therefore important to characterize their structures and topologies at an atomic

level. The aggregation is highly dynamic, however, and atomic insights from experimental data are difficult to obtain. In this context, computer simulation is an interesting approach to go where experiments have failed thus far and can serve as a basis for further experimental studies.

In a previous article of this series, we describe the use of the activation-relaxation technique (ART nouveau) (12, 13) coupled with the coarse-grained OPEP energy model (14, 15) to study in detail the mechanisms of aggregation of several amyloid-forming peptides in settings varying from dimers to dodecamers (16-20). ART differs from standard Monte Carlo simulations (21) in that the ART events are defined directly in the space of configurations allowing for the generation of moves of any complexity. ART also differs from molecular dynamics (MD) in that its efficiency is not related to the height of the energy barrier at the transition point, allowing the system to move through the configuration space rapidly, without having to wait for the rare thermal fluctuations to occur as in MD simulations.

ART-OPEP simulations show that the predicted lowest energy structures of the dimer and trimer of the beta-amyloid protein fragment spanning residues 16-22 (Abeta (16-22) superpose within 1Å root-mean square deviation (rmsd) from their conformations in the fibrils determined by solid-state NMR (22). Note there is still some uncertainty about the real structures in the amyloid state. Solid-state NMR provides atomic distances only with great difficulty and therefore the current structures are models, rather than fully validated experimental conformations. On the other hand, X-ray methods provide fully reliable structures, but it remains to be determined whether the fibril states in microcrystals and in solution are identical. ART simulations on Abeta (16-22) also showed in-register anti-parallel beta-sheet in equilibrium with several out-of-register anti-parallel beta-sheets and reptation moves were found to allow the multi-chain system to pass from one register of H-bonds to another without any significant detachment of the chains (23, 24). Similarly, ART simulations on *n*-chains of the tetrapeptide KFFE ($n$= 6, 7 and 8) and the hexapeptide NFGAIL ($n$ = 12) revealed spontaneous formation of open beta-barrel and cross-beta structures from random states through fast and slow aggregation routes (17-20)).

While ART explores efficiently the conformational space and points to mechanisms qualitatively consistent with previous theoretical folding studies on the second beta-hairpin of protein G (25) or isotope-edited IR spectroscopy studies on the late steps of Abeta (16-22) aggregation (26), its present formulation does not respect detailed balance so ART does not converge to any well-defined thermodynamical ensemble and cannot give precise information regarding the free energy surface contrary to sampling methods such as replica-exchange MD (REMD). ART also fails to provide direct data regarding the dynamics and kinetics of aggregation.

In this article, we therefore turn to MD and REMD simulations to study two amyloid-forming peptides using the coarse-grained OPEP force field. We start with the dimer of the Abeta (16-22) peptide, a well-studied system by a number of numerical methods. This also allows us to further validate the force field in predicting the right free energy surface. From there, we can move to more complex aggregates: 4-mers and 16-mers of the Beta2m (83-89) peptide (the fragment 83-89 of human beta2-microglobulin protein). This peptide has the particularity of counting very few hydrophobic residues, which makes it possible to sample more efficiently the conformational space on a similar MD timescale as the number of attractive intermolecular interactions are reduced compared with many other amyloid-forming peptides of similar length.

REMD simulations on the dimer of the Abeta (16-22) peptide show that the system is essentially random coil, but fibril-competent conformations do exist, albeit with a low probability at room temperature. Increasing the size of the system to a tetramer does not basically change the results. MD simulations on the tetramer of the Beta2m (83-89) peptide reveal many topologies in equilibrium, including the cross-beta structure characteristic of amyloid fibrils and amorphous aggregates. Comparing the MD-OPEP and ART-OPEP simulations, we find that both methods give a similar topological picture, further validating the use of activated methods. Finally, MD simulations on the 16-mers of Beta2m (83-89) show that the self-assembly is very complicated and displays mainly disordered and highly heterogeneous topologies, but again fibril-competent and annular structures are detected with a marginal probability. These simulations show how it is possible to make progress in our understanding of protein aggregation using a multi-step approach with carefully selected simulation methods and sequences.

## 3. MATERIALS AND METHODS

### 3.1. Choice of the peptides

In this study, we focus on two amyloid-forming peptides. As a first model, we selected the dimer of the Abeta (16-22) peptide of sequence KLVFFAE for several reasons. First, the positioning of the chains in the solid-state NMR models is not constant and the register of hydrogen bonding interactions appears to vary with pH conditions, providing strong evidence of the polymorphism character of the fibrils (27). Second, this peptide in low-order species was studied by many different numerical approaches using various force fields (28-32). Notably, the free energy surface of the Abeta (16-22) dimer, determined using all-atom explicit solvent simulations (32) can be compared with simulations using the coarse-grained implicit solvent OPEP force field. Finally, although the early steps of aggregation involve various oligomeric species in dynamic equilibrium, it is useful to develop a detailed knowledge of the structural characteristics of the most populated states accessible to the dimer of a short peptide. Indeed, many short peptides form amyloids *in vitro*, such as KFFE (33), NFGAIL (34), GNNQQNY (8), STVIIE (35), DFNKF (36) and NFGSVQ (37).

As a second model, we select the Beta2m (83-89) peptide with sequence NHVTLSQ, i.e. the fragment 83-89 of human beta2-microglobulin. The beta2-microglobulin is a 99-residue protein and forms a non-covalently bound light chain of the class I major histocompatibility complex. The full-length protein can aggregate into amyloid fibrils and their deposition is thought to be the cause of dialysis-related amyloidosis, a serious complication in patients receiving long-term hemodialysis. Recently, Ivanova *et al.* discovered that the Beta2m (83-89) peptide can also form amyloid fibrils at pH 2 and 37□ with 2.0 M NaCl/25 mM phosphate (38). In contrast to Abeta (16-22), this peptide has been the subject of very few computational studies. In one of these, Lei *et al.* proposed from implicit and explicit solvent all-atom MD simulations of the dimer that anti-parallel beta-sheets were more stable than parallel sheets, but a full thermodynamic characterization was not provided (39). A longer fragment spanning 83-99 was also studied using REMD and MD simulations in explicit solvent, but only for the monomer and the dimer (40). Some more theoretical work is therefore clearly needed. Moreover, it is essential to study several peptides in order to understand the common dynamic and thermodynamic aggregation features shared by these systems using a single approach and to determine the molecular origins of variability and similarity observed in the stability of small oligomers using the various computational methods available today. In this work using MD-OPEP simulations, we first elucidate the free energy surface of the Beta2m (83-89) tetramer. Then, because larger species can represent building blocks in the fibrillization process, we report the dominant populated aggregates in the early steps of aggregation of 16 Beta2m (83-89) peptides.

### 3.2. OPEP force field

The coarse-grained implicit solvent OPEP force field has been described in detail elsewhere (14, 15). Each amino acid includes all backbone N, H, Calpha, C, and O atoms and each side chain (Sc) is modeled by a single particle with appropriate Van der Waals radius and geometry. OPEP is a generic force field that can be used for any D-amino acid sequence. Its energy function includes local terms associated with the bond lengths, bond angles, improper torsions and the backbone torsions, pair-wise contact potentials between backbone - backbone, side-chain - backbone and side-chain - side-chain particles (considering all 20 amino acid types), and backbone two-body and four-body (cooperative) hydrogen bonding interactions. Compared with other coarse-grained models used for studying protein aggregation, OPEP treats explicitly the oxygen and hydrogen atoms participating in the H-bonds, and its parameters have been trained and tested on a set of 30 proteins in solution (41). The resulting parameter set, OPEP version 3.2 used in this work, coupled with ART simulations has been shown to provide high accuracy in reproducing the equilibrium structures of the peptide Abeta (21-30) in solution (42).

### 3.3. MD and REMD with OPEP

MD simulations are performed with an in-house package, *simulateur*, developed by N.M. and P.D. (43). All simulations are carried out at neutral pH and at constant temperature controlled by the Berendsen's bath (coupling time of 0.5 ps) in spheres of size many times the length of a monomer with reflecting boundary conditions. The integration time step is 1 fs and all non-bonded interactions are updated at every step. As a first step towards determining the relationship between the OPEP-MD and experimental time scales, we use the unblocked alanine decapeptide. Although its global free energy minimum is unknown from experiment and from OPEP, we consider that folding to the full alpha-helix conformation would give a good indication of the speed up. Using a total of 20 trajectories started from fully extended or random states, we find that the average folding time at 300 K is 2.1 ns (N Mousseau and P. Derreumaux, in preparation) to be compared to 0.1-0.6 μs from experiment (44), and therefore OPEP-MD offers approximately a two-order speedup relative to experiment.

REMD is an enhanced sampling protocol in which several identical copies (replicas) of the system are run in parallel at different temperatures and are periodically swapped with a probability given by the Metropolis criterion (45). This scheme, which performs random walks in temperature space, enables the system to escape from low energy traps (runs at high T) and to explore local minima (runs at low T) (46-48). Here, the conformations of Abeta (16-22) dimer are explored using a 50-ns (at each temperature) REMD-OPEP simulation starting from two disordered chains in random orientation. Eight replicas are used with T ranging from 287 K to 500 K with exponential distribution. The exchange time between neighbouring replicas is 20 ps and the acceptance rate is on the order of 30-40%.

The 4-mers and the 16-mers of Beta2m (83-89) are subject to MD simulations at a constant T of 310 K. We perform twenty 100-ns MD runs for the 4-mers starting from a randomly chosen state. As the computational time increases with the system size, only six 100-ns MD runs are performed on the 16-mers and therefore these simulations only capture the early steps of aggregation. Using 60, 60 and 80Å diameter spheres with reflecting boundary conditions for the Abeta (16-22) dimer, the tetramer and 16-mers of Beta2m (83-89), the concentrations of the peptides are on the order of 3, 7 and 12 mM, respectively. This millimolar concentration, used in many simulations (32), is larger than the experimental concentrations in the micromolar range (20-50 μM) (22, 38), but enables us to study the aggregation mechanisms from a large number of simulations using current computer facilities.

### 3.4. Analysis of the simulations

In all simulations presented below, the first 2 ns MD or REMD simulation, and the first 1000 ART events are excluded from analysis. The free energy surfaces of the Abeta (16-22) dimer and the Beta2m (83-89) tetramer are constructed as a function of two reaction coordinates. The free energy is calculated using the standard formula:

$$F = -RT \log H(x,y$$

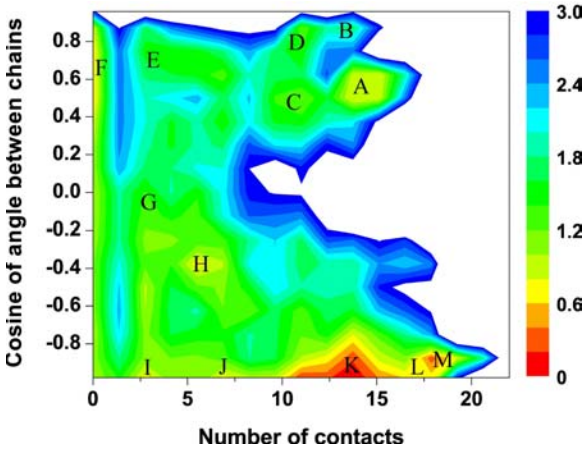


**Figure 1.** Free energy surface of the Abeta (16-22) dimer from REMD-OPEP simulation. The reaction coordinates used are the cosine of the angle between the chains and the number of intermolecular contacts between the Calpha atoms. The free energy minima in kcal/mol are labeled from A to M. Statistical errors are on the order of 0.2 kcal/mol.

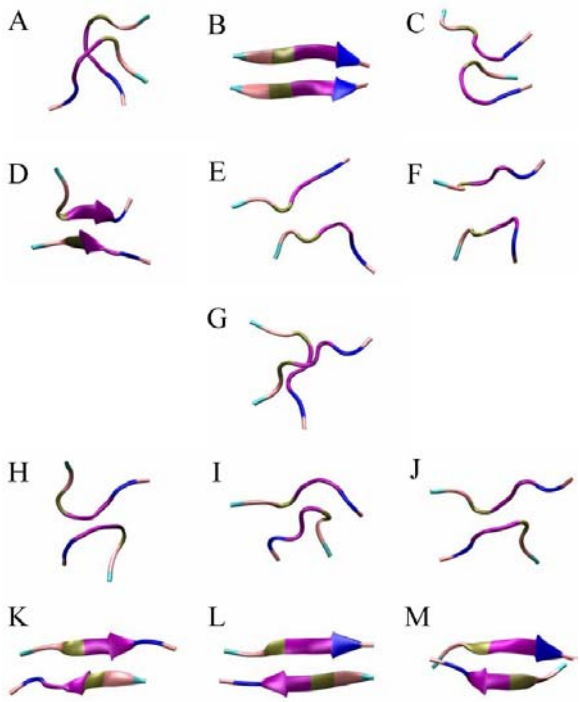


**Figure 2.** Representative Abeta (16-22) structures (in new-cartoon representation) of the free energy basins labeled in Figure 1. The color code for each amino acid is the following: Lys16 in cyan, Leu17 in pink, Val18 in tan, Phe19 and Phe20 in purple, Ala21 in blue, and Glu22 in light pink.

where $x$ and $y$ are two selected reaction coordinates, $R$ is the gas constant, $T$ is the temperature, and $H(x,y)$ is the histogram of $x$ and $y$. Umbrella sampling and thermodynamic integration techniques are not necessary for the systems under study because the MD runs overlap, indicating that equilibrium is reached.

To characterize the dominant aggregates and the aggregation process of the Abeta (16-22) dimer and Beta2m (83-89) tetramer as a function of time, we monitor the secondary structure content, the radius of gyration, the independent-chain rmsd from a selected structure, the number of inter-chain side chain – side-chain contacts, and the number of inter-chain Calpha-Calpha contacts for all the conformations. Two side chains $k$ and $l$ of Van der Waals radius $R_k$ and $R_l$ are in contact if they deviate by less than $R_k + R_l + 1$ Å (24). Two chains are considered as a parallel (anti-parallel) beta-sheet if the scalar product of the normalized end-to-end unit vector is greater than 0.7 (less than –0.7) and at least two consecutive residues of each chain visit the beta-strand state. One hydrogen bond (H-bond) is considered as formed if the N…O distance is less than 3.5 Å and the angle N-H…O is greater than 150 degrees.

To study the aggregation process of Beta2m (83-89) 16-mers, we classify the aggregates according to a family type descriptor based on the size of the beta-sheets formed and the number of chains without beta-sheet content. Here, two chains are considered to form a beta-sheet if they display at least three H-bonds and at least two consecutive residues of each chain have a beta-strand signature. For instance, an aggregate consisting of a seven-stranded beta-sheet, a five-stranded beta-sheet and four chains devoid of beta-sheet signature is described by a family type of 7 + 5 + 1 + 1 + 1 + 1 or 7 + 5 + 1×4, with 1×4 representing four chains without any beta-sheet signature.

## 4. RESULTS

### 4.1. Free energy surfaces of Abeta (16-22) dimerization

We compute the free energy surface of the Abeta (16-22) dimer, using a 50 ns REMD-OPEP simulation starting from two randomly orientated chains in random conformations. Statistical errors are calculated comparing results from the 10-30 ns and 30-50 ns time intervals.

Figure 1 shows the free energy surface of Abeta (16-22) dimer at 310 K projected on two reaction coordinates: the cosine of the angle between the two chains and the number of inter-chain Calpha contacts (less than 6.5 Å). Identical parameters were used by Gnanakaran *et al.* to generate the free energy surface of the Abeta (16-22) dimer using a modified version of the AMBER94 force field in explicit solvent (32). We find multiple free energy minima and representative structures in these basins are shown in Figure 2. In Structures A-F and H-M, the cosine of the angle between the chains is positive and negative, respectively, while in structure G, the cosine of the angle is close to zero. These structures consist of two loops (structure A), in-register and out-of-register parallel beta-sheets (structures B and D), a rather extended chain interacting with a loop (structure C), parallel disordered chains (structure E), two chains devoid of intermolecular Calpha contacts but stabilized by side-chain - side-chain

interactions (structure F), cross chains (structure G), anti-parallel loops (structure H), an extended chain and a loop with anti-parallel orientation (structure I), anti-parallel disordered chains (structure J), and in-register and out-of-register anti-parallel beta-sheets (structures K, L and M). Averaged over all conformations, the percentage of beta-strand content is 36% at 310 K using the DSSP program (49) and therefore the peptide is predicted to be random coil in solution. However, the dimer spends a non-negligible fraction of its time in relatively well-ordered free-energy basins, which may facilitate the growth of beta-sheet oligomers.

Consistent with previous simulations of the same peptide dimer using OPEP or all-atom force fields (23, 28, 29), the anti-parallel arrangement is found to be more populated than the parallel arrangement, but cross-chain conformations also exist (see structure G in Figure 2). Solid-state NMR derived fibril at neutral pH (22) indicates that the peptides form an anti-parallel beta-sheet structure described by a 16+k ↔ 22-k beta-sheet registry (i.e., intermolecular H bonds between residues 16+k and 22-k of the two chains, with k = 0, 2, 4, and 6, and the C=O…H-N and N-H…O=C H-bonds formed). The state L displays the NMR 16+k ↔ 22-k registry, while M and K show shifted registries: a 17+k ↔ 21-k registry for structure M and a 16+k ↔ 21-k registry for structure K. Overall the free energy surface we find, with in-register and out-of-register, anti-parallel and parallel beta-sheets, indicates that the energy gap between these various alignments is rather small so that the peptide length or various external conditions such as concentration, temperature, and pH could easily shift the dominant structure from one beta-sheet registry to another. This is consistent with the solid-state NMR derived structure of the Abeta (11-25) fibrils where anti-parallel beta-sheets with 17+k ↔ 20-k registry were found at pH 7.4 versus 17+k ↔ 22- k registry at pH 2.4 (27). In this context, Gordon *et al.* also showed that a change in Abeta (16-22) amphiphilicity, via the addition of an octanoyl group at the N-terminus, shifts the fibrils from anti-parallel (16+k ↔ 22+k registry) to parallel (16+k ↔ 16+k registry) beta-sheets (50).

As indicated above, the free energy surface at 310 K shows that the dimer conformation is more favorable than the two non-interacting peptides and that the chains move relatively freely with respect to each other and visit predominantly disordered states. This is not a perfectly random walk, however, and there is a clear bias towards passing through multiple assembly-competent or cross conformations, albeit with a low probability of occurrence. The origin of this bias cannot be assigned to a single factor, of course, and analysis of the intermolecular side-chain - side-chain contacts indicates that the Lys17-Glu22 interaction is present in some of the conformations while the hydrophobic Phe-Phe, Phe-Ala, Leu-Phe, Leu-Ala interactions are present in most of the ordered conformations.

Finally, we emphasize that the OPEP free energy surface shares many features with what was observed in all-atom explicit solvent simulations (see Figure 1 of Ref.32). In both simulations, the two Abeta (16-22) chains are shown to be able to adopt many different conformations: parallel and anti-parallel loops, an extended chain with a loop in parallel/anti-parallel orientation, in-/out-of-register parallel and anti-parallel beta-sheets and cross chains. This analysis along with the work reported in Refs. 41 and 42 further validates the implicit solvent OPEP force field and opens the door to the study of the free energy surfaces of higher-order species using reasonable computer resources, as reported now.

### 4.2. Thermodynamics of Beta2m (83-89) tetramer

Since it has been hypothesized that the critical nucleus could be as small as a trimer or a tetramer for the GNNQQNY peptide (8), it has become essential to develop a detailed characterization of the thermodynamic properties of small oligomers, such as tetramers, in order to assess the role of these aggregates. In particular, given the strongly out-of-equilibrium nature of the fibrillization process, it is not clear whether these small aggregates play the role of building blocks, from which the fibril grows, or if they are a real critical nucleus in the sense of nucleation theory. At the moment, answers to these questions are far from clear.

While the free energy surface was shown to vary from dimers to tetramers using on-lattice models (51), very conflicting conclusions were drawn from stability studies of tetramers using all-atom MD simulations. In large part, therefore, the question remains open regarding the nature of the free energy surface of small oligomers. In their on-lattice 64-amino acid peptide model simulation, Cellmer *et al.* found that the free-energy landscape shows an increased preference for misfolded states as the number of chains goes up (51). Based on all-atom simulations of DFNKF oligomers in a confined box, Tsai et al. found, on the contrary, that tetrameric beta-sheets are stable in 10-ns MD simulations and their stability increases with their size (52). Similarly Lai et al. found that a four-stranded beta-sheet is a dominant topology for the GNNQQNY peptide starting from a preformed three-stranded beta-sheet and one random chain within a time scale of 80 ns using the Gromos96 force field (53).

On the other hand, Paci *et al.* (54) and Mousseau and Derreumaux (20, 55), did not find any evidence for the thermodynamic predominance of such ordered structures in trimers and tetramers of TTR (105-115) and related peptides, using implicit solvent models and starting from a random initial state. In fact, we see that simple models or implicit solvent simulations favor disordered structures, while explicit solvent simulations tend to demonstrate the stability of the ordered arrangements starting from ordered structures. This suggests that the discrepancy could be due to the lack of convergence of the more costly all-atom explicit solvent simulations. It could also support the building block concept: while a perfectly ordered small oligomer is a rare event, once it is formed, its stability is such that it will remain in solution for a long time and clearly ease the growth of ordered amyloid structures.

To determine the thermodynamics and aggregation paths of the Beta2m (83-89) peptide, we use two distinct computer methodologies coupled with the OPEP energy model: ART nouveau and MD. As reported

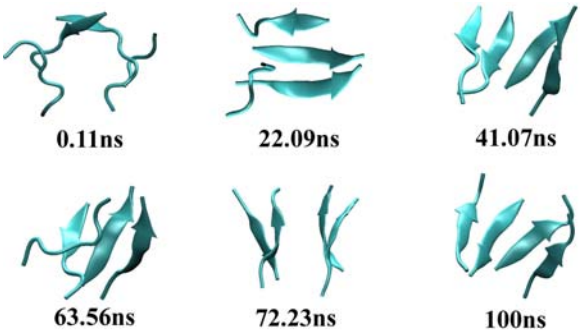


**Figure 3.** Snapshots of a MD run of the Beta2m (83-89) tetramer at 310 K starting from a ring-like state. After 22 ns, the ring has broken and a three-stranded beta-sheet is formed. At 41 ns, the last chain allows for the formation of a four-stranded beta-sheet with mixed orientations. This arrangement breaks again at 63 ns. The sampling continues as the system forms a bi-layer beta-sheet at 72 ns that converts into another four-stranded beta-sheet at 100 ns.

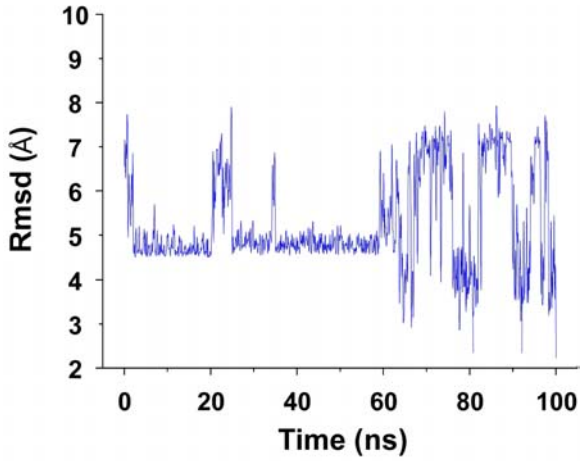


**Figure 4.** Time evolution of the Calpha-rmsd with respect to the final structure (t=100 ns) for the MD run shown in Figure 3. Note that the final structure is explored several times between 60-100 ns. All points are averaged over 50 ps.

in the previous articles of this series, each ART event brings the system from one relaxed state to another, going through an activation barrier, and accepts or rejects the move according to the Metropolis criterion. ART offers an efficient sampling of low energy conformations, though it is not designed to provide accurate thermodynamics. Comparing ART and MD results, we can ensure that the free-energy surface is well converged and that it does not miss any significant basins.

Here, we perform ten 18,000-event ART trajectories starting from a randomly chosen orientation and conformation of the chains, at a Metropolis temperature of 1200 K to establish the range of low-energy structures (the Metropolis temperature cannot be compared to a physical temperature since ART accept/reject moves do not include vibrational entropic contributions). We also run twenty independent 100-ns MD simulations at 310 K starting from the same random state (15 runs) or a ring-like conformation (5 runs).

Figure 3 shows representative snapshots along a MD run starting from a ring-like state. The dynamics is rich and the system samples, in the course of 100 ns, a four-stranded monolayer beta-sheet, one extended chain located above the plane of a three stranded beta-sheet, and a bi-layer two-stranded beta-sheet. Figure 4, which plots the Calpha rmsd with respect to the final generated structure, shows that the mixed parallel/anti-parallel monolayer beta-sheet is explored several times (with rmsd less than 2 Å) between 60 and 100 ns, suggesting that the sampling is fully equilibrated.

Figure 5A shows the distribution density surface generated by ART as a function of the radius of gyration of the Calpha atoms and that of the side-chain beads. This surface, which is not a free energy surface, can be described by five families of structures, based on the rmsd-based clustering of all conformations. These include from left to right in Figure 5: a mixed parallel and anti-parallel twisted four-stranded beta-sheet, amorphous aggregates, ring-like conformations, a three-stranded beta-sheet stabilized by one extended chain located above the plane of the beta-sheet, and a bi-layer beta-sheet. There is no experimental data to validate the predicted preference for parallel beta-strands, but the ordered bi-layer beta-sheet with Calpha…Calpha distances of 5.0 Å between the strands and 11.0 Å between the layers is consistent with the crystal structure of the cross-beta spine model formed by the peptide GNNQQNY (8). In addition, the twist of the four stranded beta-sheet is fully consistent with all-atom MD simulations in explicit solvent (56).

Figure 5B gives now the free energy surface generated from 2.0 μs MD-OPEP simulations at 310 K using the same order parameters. While we observe deviations from the ART-generated landscape — the values of the radii of gyration are 0.5 Å larger because of thermal fluctuations — the overall picture remains identical, with architectures ranging from amorphous and ring-like conformations to beta-sheets, indicating that MD has not been trapped in metastable states but also that ART simulations capture the essential features of the free-energy landscape even though its sampling is not thermodynamically defined. Note that for simplicity, we only show in Figure 5 the parallel bi-layer beta-sheet (but orthogonal beta-sheets exist), and the monolayer beta-sheet with parallel chains (but various H-bond registries and mixed parallel/anti-parallel arrangements exist). This multiplicity of H-bond registers and orientations of the chains is consistent with explicit MD simulations on related short-peptides (57).

Overall the population of beta-sheet content is 42% (vs. 58% of random coil) at 310 K by using the DSSP program (49) and the dominant species are in dynamic equilibrium. These findings suggest that four Beta2m (83-89) peptides would be assigned as random coils by CD, if they could be separated from the other species by

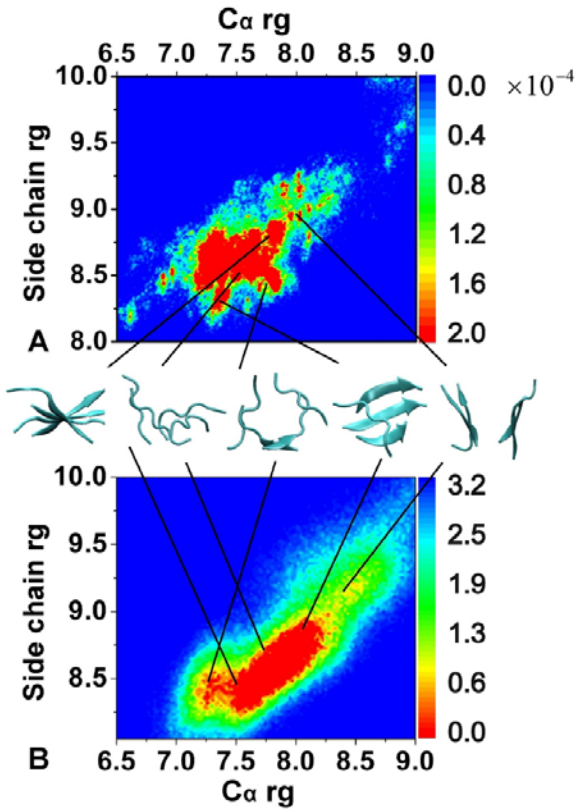


**Figure 5.** Energy landscapes of Beta2m (83-89) tetramer (A) Distribution density surface using ART. (B) Free energy surface (in kcal/mol) at 310 K from MD. Both surfaces are plotted as function of the radii of gyration (rg) of the backbone Calpha atoms and the side-chain beads. Statistical errors are on the order of 3%.

ultracentrifugation, dynamic light scattering or Photoinduced Cross-Linking of Unmodified Proteins techniques (PICUP) (58, 59) even though there is a non-negligible population of beta-sheet structures.

Figure 6 shows the probability map of inter-peptide side-chain - side-chain contacts within the four typical structures at 310 K. The contact probability is calculated on a subset of 6000 conformations for each structure. All these 6000 conformations are taken from the same MD run and have Calpha rmsd less than 4 Å with respect to the structure shown in Figure 6. The registry and the orientation of the beta-strands in the beta-sheet can be clearly seen from the contact probability map. For the bi-layer beta-sheet structure (Figure 6A), there are 6 main contact areas. The two larger areas represent the side-chain - side-chain contacts between the strands within each sheet, while the other areas represent the contacts between the sheets. The contact map also shows that chains 1 and 2 forms one sheet and chains 3 and 4 forms the other sheet. From the five red-circled contacts located in the lower-left area of the map and the five red-circled contacts located in the upper-right area, we see that both beta-sheets are in-register anti-parallel. The four areas with three red-circled contacts are the Leu-Leu, Val-Val and Leu-Val hydrophobic interactions which stabilize the two layers. Similarly, in the monolayer beta-sheet (Figure 6B) , the four strands are all parallel and in-register, although only parts of the chains form the beta-sheet. In the three-stranded beta-sheet with one extended chain located above the plane of the sheet (Figure 6C), the three strands (chains 3 1 4) are parallel, chains 1 and 4 are in-register, while chains 3 and 1 are out-of-register. Strong hydrophobic interactions between chain 2 and chains 3, 1 and 4 are seen in the map. In the ring-like organization (Figure 6D), all the strands are rather anti-parallel and out of register. Taken together, each structure is stabilized by a unique pattern of physical interactions, although the hydrophobic residues form the most common contacts.

Remarkably, all the three organizations with high-beta sheet content described here for a tetramer of Beta2m (83-89) were observed on multiple chains of KFFE, Abeta (16-22), Abeta (11-25) and GNNQQNY using various simulations and force fields (16, 17, 23, 43, 55). For instance, both all-atom MD on the tetramer of GNNQQNY and OPEP-MD on the tetramer of Abeta (16-22) showed a transition between the bi-layer beta-sheet and the three-stranded beta-sheet stabilized by a monomer (43, 53). All together these simulations point to the universality and independence of the structural characteristics of tetramers for short peptides. This is not totally surprising, because the existence of alpha-helices and beta-strands was derived from simple geometrical consideration of the peptide bonds and hard-sphere resolution (60, 61). It remains to be determined how the population of the dominant states and the dynamics from random to folded states are affected by the details of the side chains and solvent conditions.

### 4.3. Following the early steps of 16 Beta2m (83-89) chains aggregation

Understanding the thermodynamics and dynamics associated with the aggregation of many chains is a challenging problem. Colombo *et al.* used all-atom MD simulations to study the initial self-assembly stages of the $NH_2$-NFGAIL-COOH peptide, the core-recognition motif of the type II diabetes associated with islet amyloid polypeptide. Their trajectories, performed using 26 chains in a water box starting from a random distribution of the peptides, display an increase of amino acids with beta-strand character, but only amorphous aggregates were explored within a time scale of 10 ns (62). Using implicit solvent DMD simulations coupled with a low-resolution protein model, Nguyen *et al.* monitored the aggregation of 48 Ac-$KA_{14}K$-$NH_2$ chains. They found that the formation of small amorphous aggregates precedes ordered nucleus formation and that the subsequent rapid fibril growth takes place through the addition of beta-sheets laterally and monomeric peptides at the fibril-ends (63). Whether the generated dynamics and thermodynamics reflect reality remains to be determined. For their part, Dokholyan *et al.* studied the length dependence of the polyQ-mediated protein aggregation using implicit solvent DMD simulations with a simplified model including the N, Calpha, C and O backbone atoms and optional side-chain

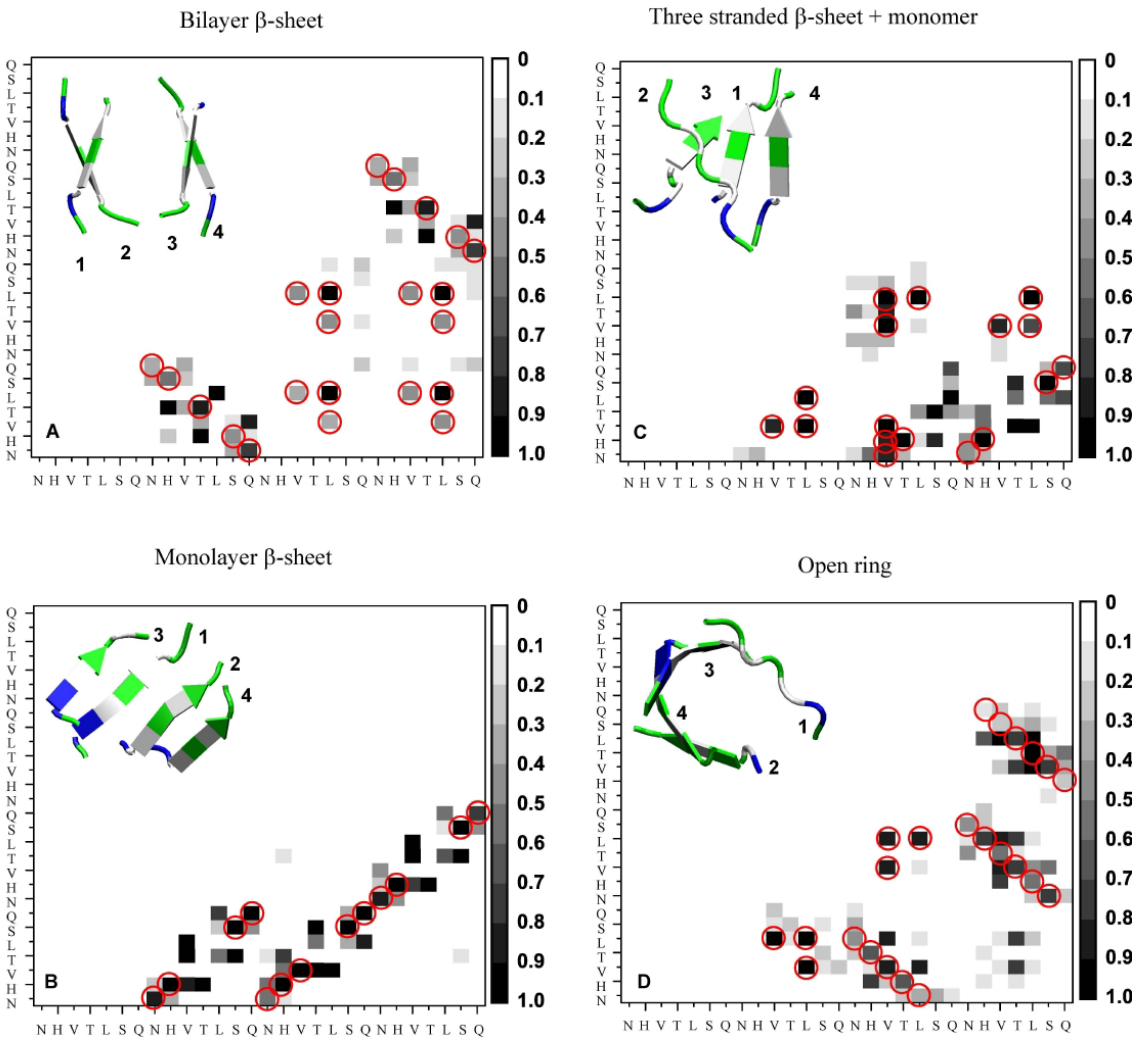


**Figure 6.** Probability map of each Sc – Sc contact within the four dominant topologies of the Beta2m (83-89) 4-mers. The four chains are labeled. Contacts, used to recognize the beta-sheet register, are indicated by a red circle.

beads depending on the residue type (64). Other coarse-grained models have been recently introduced. Pellarin and Caflisch proposed a Calpha-Cbeta model (65) while Bellesia and Shea (66) introduced a X-Y-Sc model for each amino acid, where X and Y represent two backbone groups and Sc one group for the side chain. Both models form cross-beta structures in Langevin dynamics simulations, but the interpretation of the kinetics and thermodynamics again remain to be validated using more realistic chain representations and force fields. We believe that OPEP is more realistic because it treats explicitly all atoms participating in H-bonds (neglected in all other coarse-grained model for protein aggregation), and its parameters have been trained and tested on monomeric proteins and not on amyloid-forming sequences.

Using a total of six independent 100-ns OPEP-MD runs of the Beta2m (83-89) 16-mer at 310 K starting from random states (Figure 7) where each disordered chain is separated from each other by more than 9 Å, we first characterize the population of the dominant aggregates using the classification type described in Section 3.4, i.e., by simply counting how many chains have a beta-sheet conformation in each snapshot.

The classification of the whole dataset consisting of 60,000 conformations leads to 171 families in total. This number is much smaller, but also much more significant than that derived from a standard RMSD-based clusterization as it focuses on the topological elements. This is especially true here because the RMSD between some members of the same family can reach 12 Å, emphasizing the diversity of conformations explored in the early steps of aggregation. The ten most populated families representing 42% of the conformations explored are given in table 1 (these populations must be considered as indicative only, because in contrast to the dimer and tetramer studies, the simulations do not converge to equilibrium). These ten aggregates, which consist of

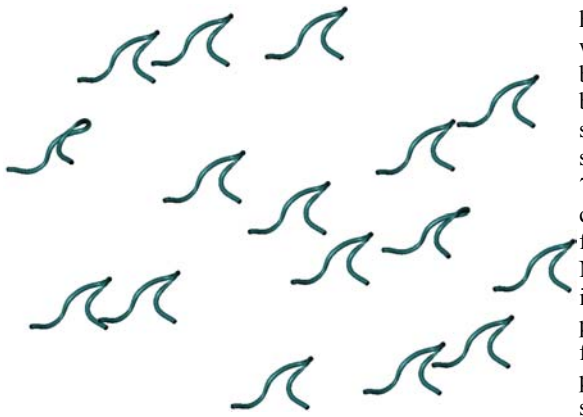

**Figure 7.** Initial state for the MD simulations of 16 Beta2m (83-89) peptides.

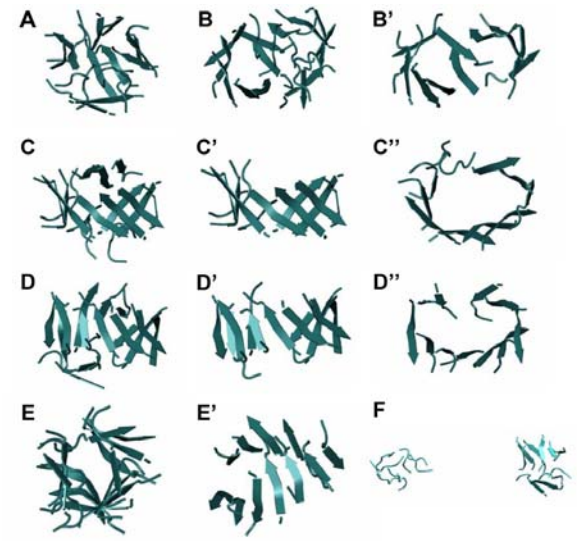


**Figure 8.** Representative aggregates explored by MD-OPEP of 16 Beta2m (83-89) peptides. For clarity, structures B', C' and D' only depict 11 chains. Structures B', C'', D'' and E' provide other views of B, C', D' and E, respectively.

mixtures of two-, three- and four-stranded beta-sheets, are not random coil, but rather assemble into globular amorphous states. Structure A in Figure 8 depicts such a state of family type 3+2+2+2+1×7 belonging to the family number 3 in Table 1. Such a high percentage of amorphous aggregates with non-negligible beta-sheet content are consistent with what has been observed for many proteins in the early steps of aggregation.

Remarkably, if we look at aggregates with much lower probabilities (on the order of 0.1%), we find that the chains form either 16-meric aggregates (structures B-E' in Figure 8) or a mixture of hexamers and decamers (Structure F).

Structural diversity in the 16-meric aggregates is, however, observed. When the network of H-bonds is less heterogeneous, structural rearrangements become easier, as would be expected, and the system adopts shapes that can be characterized as prototypical of bi-layer beta-sheets, beta-barrels or ring-like structures. Representative structures of these aggregates, labeled as structures B-E, are shown in Figure 8. Structure B has a family type of 7+4+2+1×3 where the seven-stranded beta-sheet displays a closed beta-barrel structure and the four-stranded beta-sheet forms an open ring. The 7+4 part is shown in Figure 8 B'. Note that a closed seven-stranded beta-barrel was observed in MD-OPEP simulations of seven Beta2m (83-89) peptides (unpublished results) and section 4.2. reports the finding of open rings for the tetramer of Beta2m (83-89), providing strong evidence that populated aggregates in smaller species can act as seeds for polymerization. The structures C and D are characterized by a family type of 7+4+3+2 and 7+3+2+1×4, respectively. Both of them display a beta-barrel and the 11 chains forming the beta-barrel are shown in C' and D'. Other views of the C' and D' structures are shown in C'' and D''. Finally, structure E is described by a family type of 7+4+3+1×2 and is characterized by a bi-layer beta-sheet consisting of a four-stranded beta-sheet and a seven-stranded beta-sheet. Another view of E is shown in E'.

To follow the aggregation of the 16 Beta2m (83-89) peptides, we monitor the time evolution of the size of the biggest beta-sheet formed in one MD trajectory. As seen in Figure 9, the biggest cluster rapidly evolves from a two-stranded beta-sheet to a 11-stranded beta-sheet, then breaks apart down and fluctuates essentially between a two- and eight-stranded beta-sheet. This fluctuation shows that the a 16-chain system does not form (at least within the number of simulations used here) directly a protofibril, which would likely be stable if we had started from it, but rather explores a large number of various conformations, a sampling that is likely to be preferable from a free-energy point of view. These results are preliminary and we need to pursue our simulations much beyond the MD-OPEP μs time scale (equivalent to 0.1 ms experimentally) in order to have a chance to see more ordered organizations.

## 5. CONCLUSIONS

Following the aggregation of amyloid proteins at an atomic level is a challenge experimentally because the process is very complex and sensitive to external conditions. Theoretical studies and simulations offer the possibility to understand the aggregation (20, 67-69). All *in-silico* protocols have advantages, but also have limitations. In this report, after demonstrating that the free energy surface of the Abeta (16-22) dimer obtained with the coarse-grained OPEP force field is very similar to that derived from all-atom models with explicit solvent, we study the Beta2m (83-89) peptide and characterize the free energy surface of tetramers and the early steps of the aggregation of 16-mers. Using MD-OPEP simulations at 310 K, our main findings can be summarized as follows. 1) Both the cross-beta structure and the amorphous oligomers reported experimentally for many proteins are encoded at the tetrameric level. The peptide is however essentially random coil, suggesting that the nucleus size from which

**Table 1.** The ten predicted dominant aggregates of 16 Beta2m (83-89) chains with their family types and populations

| Families | Family type | Population |
|---|---|---|
| 1 | 3+2+2+1×9 | 7.5% |
| 2 | 3+3+2+2+1×6 | 5.7% |
| 3 | 3+2+2+2+1×7 | 5.4% |
| 4 | 3+2+1×11 | 4.8% |
| 5 | 3+3+2+1×8 | 4.3% |
| 6 | 3+3+2+2+2+1×4 | 3.7% |
| 7 | 4+3+3+2+1×4 | 3.1% |
| 8 | 4+3+2+2+1×5 | 2.6% |
| 9 | 3+2+2+2+2+1×5 | 2.6% |
| 10 | 4+3+2+1×7 | 2.6% |

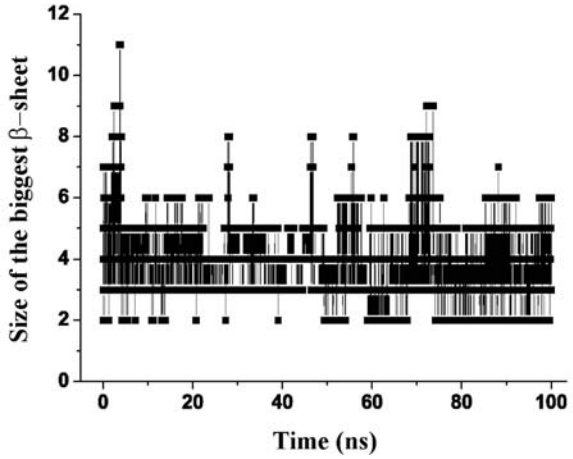


**Figure 9.** Time evolution of the size of the biggest beta-sheet formed in the aggregates generated by one 100-ns MD-OPEP simulation of 16 Beta2m (83-89) peptides.

rapid fibril growth occurs exceeds four chains for this peptide. Of course, the size of the critical nucleus clearly depends on the conditions used in the experiments or in the simulations but due to the high-effective concentration, this result should be a clear lower-bound (65, 68). 2) The early formed aggregates of 16 chains are highly-heterogeneous in structure, implying that the free energy surface is more complex than expected and there are many kinetic traps. The majority of these aggregates are amorphous consistent with experimental studies. The fact that the 16-mers constantly move from one structure to another is also fully consistent with the long lag phase measured experimentally. Remarkably, we also find aggregates with beta-barrel, open ring and bi-layer beta-sheet character, albeit with a low probability. It remains to be determined whether and how these aggregates can further grow into cross-beta structures, and which oligomeric species are cytotoxic (69). A combination of experimental and computational studies will allow develop new efficient inhibitors for Alzheimer's disease, affecting today more than 15 million people world-wide.

## 6. ACKNOWLEDGMENTS

This work is funded by NSFC (Grant No.10674029), the Young Foundation and the Senior Visiting Scholar Grant of Fudan University, NSERC, CRC, CNRS and the Université of Paris7 Denis-Diderot. We are grateful to the Réseau québécois de calcul de haute performance, Shanghai Supercomputing Center and the National High Performance Computing Center of Fudan University.

## 7. REFERENCES

1. Selkoe, D. J.: The cell biology of beta-amyloid precursor protein and presenilin in Alzheimer's disease. *Trends. Cell. Biol.*, 7, 447-453 (1998)
2. Dobson, C.: Protein folding and misfolding. *Nature*, 426, 884-890 (2003)
3. Ross, C. A. and M. A. Poirier: Protein aggregation and neurodegenerative disease. *Nat. Med.*, 10, S10-S17 (2004)
4. Chiti, F. and C. Dobson: Protein misfolding, functional amyloid, and human disease. *Ann. Rev. Biochem.*, 75, 333-366 (2006)
5. Zhang, S., K. Iwata, M. J. Lachenmann, J. W. Peng, S. Li, E. R. Stimson, Y. A. Lu, A. M. Felix, J. E. Maggio and J. P. Lee: The Alzheimer's peptide A beta adopts a collapsed coil structure in water *J. Struct. Biol.*, 130, 130-141 (2000)
6. Zahn, R., A. Liu, T. Luhrs, R. Riek, C. von Schroetter, F. L. Garcia, M. Billeter, C. L., G. Wider and K. Wuthrich: NMR solution structure of the human prion protein. *Proc. Natl. Acad. Sci. U.S.A.*, 97, 145-150 (2000)
7. Sunde, M., L. Serpell, M. Bartlam, P. Fraser, M. Pepys and C. Blake: Common core structure of amyloid fibrils by synchrotron x-ray diffraction. *J. Mol. Biol.*, 273, 729-739 (1997)
8. Nelson, R., M. R. Sawaya, M. Balbirnie, A. O. Madsen, C. Riekel, R. Grothe and D. Eisenberg: Structure of the cross-beta spine of amyloid-like fibrils. *Nature*, 435, 773-778 (2005)
9. Walsh, D. M., I. Klyubin, J. V. Fadeeva, W. K. Cullen, R. Anwyl, M. S. Wolfe, M. J. Rowan and D. J. Selkoe: Naturally secreted oligomers of amyloid beta protein potently inhibit hippocampal long-term potentiation *in vivo*. *Nature*, 416, 483-484 (2002)
10. Lesne, S., M. Teng Koh, L. Kotilinek, R. Kayed, C. G. Glabe, A. Yang, M. Gallaher and K. H. Ashe: A specific amyloid-beta protein assembly in the brain impairs memory. *Nature*, 440, 352-357 (2006)
11. Pastor, M. T., N. Kümmerer, V. Schubert, A. Esteras-Chopo, C. G. Dotti, M. López de la Paz and L. Serrano: Amyloid toxicity is independent of polypeptide sequence, length and chirality. *J. Mol. Biol.*, in press, (2007)
12. Malek, R. and N. Mousseau: Dynamics of Lennard-Jones clusters: A characterization of the activation-relaxation technique. *Phys Rev E Stat Phys Plasmas Fluids Relat Interdiscip Topics*, 62, 7723-7728 (2000)
13. Wei, G., N. Mousseau and P. Derreumaux: Exploring the energy landscape of proteins: A characterization of the activation-relaxation technique. *J Chem Phys*, 117, 11379-11387 (2002)
14. Derreumaux, P.: From polypeptide sequences to structures using Monte Carlo simulations and an optimized potential. *J. Chem. Phys.*, 111, 2301-2310 (1999)

15. Derreumaux: Generating ensemble averages for small proteins from extended conformations by Monte Carlo simulations. *Phys. Rev. Lett.*, 85, 206-209 (2000)
16. Boucher, G., N. Mousseau and P. Derreumaux: Aggregating the amyloid Abeta (11-25) peptide into a four-stranded beta-sheet structure. *Proteins*, 65, 877-888 (2006)
17. Wei, G., N. Mousseau and P. Derreumaux: Sampling the self-assembly pathways of KFFE hexamers. *Biophys. J.*, 87, 3648-3656 (2004)
18. Melquiond, A., N. Mousseau and P. Derreumaux: Structures of soluble amyloid oligomers from computer simulations. *Proteins*, 65, 180-191 (2006)
19. Melquiond, A., J. C. Gelly, N. Mousseau and P. Derreumaux: Probing amyloid fibril formation of the NFGAIL peptide by computer simulations. *J Chem Phys*, 126, 065101 (2007)
20. Mousseau, N. and P. Derreumaux: Exploring the early steps of amyloid peptide aggregation by computers. *Acc. Chem. Res.*, 38, 885-891 (2005)
21. Derreumaux, P.: Folding a 20 amino acid alpha beta peptide with the diffusion-controlled Monte Carlo method. *J. Chem. Phys.*, 107, 1941-1947 (1997)
22. Balbach, J. J., Y. Ishii, O. N. Antzutkin, R. D. Leapman, N. W. Rizzo, F. Dyda, J. Reed and R. Tycko: Amyloid fibril formation by A beta 16-22, a seven-residue fragment of the Alzheimer's beta-amyloid peptide, and structural characterization by solid state NMR. *Biochemistry*, 39, 13748-13759 (2000)
23. Santini, S., G. Wei, N. Mousseau and P. Derreumaux: Pathway complexity of Alzheimer's beta-amyloid A beta (16-22) peptide assembly. *Structure*, 12, 1245-1255 (2004)
24. Santini, S., N. Mousseau and P. Derreumaux: In silico assembly of Alzheimer's Abeta (16-22) peptide into beta-sheets. *J. Am. Chem. Soc.*, 126, 11509-11516 (2004)
25. Wei, G., N. Mousseau and P. Derreumaux: Complex folding pathways in a simple beta-hairpin. *Proteins*, 56, 464-474 (2004)
26. Petty, S. A. and S. M. Decatur: Experimental evidence for the reorganization of beta-strands within aggregates of the Abeta (16-22) peptide. *J. Am. Chem. Soc.*, 127, 13488-13489 (2005)
27. Petkova, A. T., G. Buntkowsky, F. Dyda, R. D. Leapman, W. M. Yau and R. Tycko: Solid state NMR reveals a pH-dependent antiparallel beta-sheet registry in fibrils formed by a beta-amyloid peptide. *J. Mol. Biol.*, 335, 247-260 (2004)
28. Hwang, W., S. Zhang, R. D. Kamm and M. Karplus: Kinetic control of dimer structure formation in amyloid fibrillogenesis. *Proc. Natl. Acad. Sci. U.S.A.*, 101, 12916-12921 (2004)
29. Klimov, D. and Thirumalai: Dissecting the assembly of Abeta16-22 amyloid peptides into antiparallel beta sheets. *Structure*, 11, 295-307 (2003)
30. Favrin, G., A. Irback and S. Mohanty: Oligomerization of amyloid Abeta16-22 peptides using hydrogen bonds and hydrophobicity forces. *Biophys. J.*, 87, 3657-3664 (2004)
31. Rohrig, U. F., A. Laio, N. Tantalo, M. Parrinello and R. Petronzio: Stability and structure of oligomers of the Alzheimer peptide Abeta16-22: from the dimer to the 32-mer. *Biophys. J.*, 91, 3217-3229 (2006)
32. Gnanakaran, S., R. Nussinov and A. E. Garcia: Atomic-level description of amyloid beta-dimer formation. *J. Am. Chem. Soc.*, 128, 2158-9 (2006)
33. Tjernberg, L., W. Hosia, N. Bark, J. Thyberg and J. Johansson: Charge attraction and beta propensity are necessary for amyloid fibril formation from tetrapeptides. *J. Biol. Chem.*, 277, 43243-43246 (2002)
34. Tenidis, K., M. Waldner, J. Bernhagen, W. Fischle, M. Bergmann, M. Weber, M. L. Merkle, W. Voelter, H. Brunner and A. Kapurniotu: Identification of a penta- and hexapeptide of islet amyloid polypeptide (IAPP) with amyloidogenic and cytotoxic properties. *J. Mol. Biol.*, 295, 1055-1071 (2000)
35. Serrano, L.: Sequence determinants of amyloid fibril formation. *Proc. Natl. Acad. Sci. U.S.A.*, 101, 87-92 (2004)
36. Reches, M., Y. Porat and E. Gazit: Amyloid fibril formation by pentapeptide and tetrapeptide fragments of human calcitonin. *J. Biol. Chem.*, 277, 35475-35480 (2002)
37. Reches, M. and E. Gazit: Amyloidogenic hexapeptide fragment of medin: Homology to functional islet amyloid polypeptide fragments. *Amyloid*, 11, 81-89 (2004)
38. Ivanova, M. I., M. R. Sawaya, M. Gingery, A. Attinger and D. Eisenberg: An amyloid-forming segment of beta2-microglobulin suggests a molecular model for the fibril. *Proc. Natl. Acad. Sci. U. S. A.*, 101, 10584-10589 (2004)
39. Lei, H., C. Wu, Z. Wang and Y. Duan: Molecular dynamics simulations and free energy analyses on the dimer formation of an amyloidogenic heptapeptide from human beta2-microglobulin: implication for the protofibril structure. *J. Mol. Biol.*, 356, 1049-1063 (2006)
40. Liang, C., P. Derreumaux and G. Wei: Structure and aggregation mechanism of beta2 microglobulin (83-99) peptides studied by molecular dynamics simulations. *Biophys. J.*, 93, 3353-3362 (2007)
41. Maupetit, J., P. Tuffery and P. Derreumaux: A coarse-grained protein force field for folding and structure prediction. *Proteins*, 69, 394-408 (2007)
42. Chen, W., N. Mousseau and P. Derreumaux: The conformations of the amyloid-beta (21-30) fragment can be described by three families in solution. *J. Chem. Phys.*, 125, 084911-084918 (2006)
43. Derreumaux, P. and N. Mousseau: Coarse-grained protein molecular dynamics simulations. *J. Chem. Phys.*, 126, 025101 (2007)
44. Kubelka, J., J. Hofrichter and W. A. Eaton: The protein folding 'speed limit'. *Curr. Opin. Struct. Biol.*, 14, 76-88 (2004)
45. Sugita, Y. and Y. Okamoto: Replica-exchange molecular dynamics method for protein folding. *Chem. Phys. Lett.*, 314, 141-151 (1999)
46. Zhou, R., B. Berne and R. Germain: The free energy landscape for beta hairpin folding in explicit water. *Proc. Natl. Acad. Sci. U.S.A.*, 98, 14931-149316 (2001)
47. Garcia, A. E. and J. N. Onuchic: Folding a protein in a computer: an atomic description of the folding/unfolding of protein A. *Proc. Natl. Acad. Sci. U.S.A.*, 100, 13898-13903 (2003)
48. De Simone, A., A. Zagari and P. Derreumaux: Structural and hydration properties of the partially unfolded states of the prion protein. *Biophys. J.*, 93, 1284-1292 (2007)

49. Kabsch, W. and C. Sander: Dictionary of protein secondary structure: pattern recognition of hydrogen-bonded and geometrical features. *Biopolymers.*, 22, 2577-2637 (1983)
50. Gordon, D. J., J. J. Balbach, R. Tycko and S. C. Meredith: Increasing the amphiphilicity of an amyloidogenic peptide changes the beta-sheet structure in the fibrils from antiparallel to parallel. *Biophys. J.*, 86, 428-434 (2004)
51. Cellmer, T., D. Bratko, J. M. Prausnitz and H. Blanch: Protein-folding landscapes in multichain systems. *Proc. Natl. Acad. Sci. U.S.A.*, 102, 11692-11697 (2005)
52. Tsai, H. H., D. Zanuy, N. Haspel, K. Gunasekaran, B. Ma, C. J. Tsai and R. Nussinov: The stability and dynamics of the human calcitonin amyloid peptide DFNKF. *Biophys. J.*, 87, 146-158 (2004)
53. Zheng, Z., H. Chen, H. Bai and L. Lai: Molecular dynamics simulations on the oligomer-formation process of the GNNQQNY peptide from yeast prion protein Sup35. *Biophys. J.*, 93, 1484-1492 (2007)
54. Paci, E., J. Gsponer, X. Salvatella and M. Vendruscolo: Molecular dynamics studies of the process of amyloid aggregation of peptide fragments of transthyretin. *J. Mol. Biol.*, 340, 555-569 (2004)
55. Melquiond, A., G. Boucher, N. Mousseau and P. Derreumaux: Following the aggregation of amyloid forming peptides by computer simulations. *J. Chem. Phys.*, 122, 174904 (2005)
56. Esposito, L., C. Pedone and L. Vitagliano: Molecular dynamics analyses of cross-beta-spine steric zipper models: beta-sheet twisting and aggregation. *Proc. Natl. Acad. Sci. U.S.A.*, 103, 11533-11538 (2006)
57. Lopez de la Paz, M., G. M. de Mori, L. Serrano and G. Colombo: Sequence dependence of amyloid fibril formation: insights from molecular dynamics simulations. *J. Mol. Biol.*, 349, 583-596 (2005)
58. Fancy, D. A. and T. Kodadek: Chemistry for the analysis of protein protein interactions: Rapid and efficient cross-linking triggered by long wavelength light. *Proc. Natl. Acad. Sci. U.S.A.*, 96, 6020-6024 (1999)
59. Bitan, G. and D. B. Teplow: Rapid photochemical cross-linking--a new tool for studies of metastable, amyloidogenic protein assemblies. *Acc. Chem. Res.*, 37, 357-364 (2004)
60. Pauling, L. and R. B. Corey: Configuration of polypeptide chains. *Nature*, 168, 550-551 (1951)
61. Ramachandran, G. N., C. Ramakrishnan and V. Sasisekharan: Stereochemistry of polypeptide chain configurations. *J. Mol. Biol.*, 7, 95-99 (1963)
62. Colombo, G., I. Daidone, E. Gazit, A. Amadei and A. Di Nola: Molecular dynamics simulation of the aggregation of the core-recognition motif of the islet amyloid polypeptide in explicit water. *Proteins*, 59, 519-527 (2005)
63. Nguyen, H. D. and C. K. Hall: Molecular dynamics simulations of spontaneous fibril formation by random-coil peptides. *Proc. Natl. Acad. Sci. U.S.A.*, 101, 16180-16185 (2004)
64. Barton, S., R. Jacack, S. D. Khare, F. Ding and N. V. Dokholyan: The length dependence of the polyQ-mediated protein aggregation. *J. Biol. Chem.*, 282, 25487-25492 (2007)
65. Pellarin, R. and A. Caflisch: Interpreting the aggregation kinetics of amyloid peptides. *J. Mol. Biol.*, 360, 882-892 (2006)
66. Bellesia, G. and J. E. Shea: Self-assembly of beta-sheet forming peptides into chiral fibrillar aggregates. *J. Chem. Phys.*, 126, 245104-245111 (2007)
67. Ma, B. and R. Nussinov: Simulations as analytical tools to understand protein aggregation and predict amyloid conformation. *Curr. Opin. Chem. Biol.*, 10, 445-452 (2006)
68. Auer, S., C. Dobson and M. Vendruscolo: Characterization of the nucleation barriers for protein aggregation and amyloid formation. *HFSP Journal*, 1, 137-146 (2007)
69. Cheon, M., I. Chang, S. Mohanty, L. M. Luheshi and C. M. Dobson: Structural reorganization and potential toxicity of oligomeric species formed during the assembly of amyloid fibrils. *PLoS. Comput. Biol.*, 3, 1727-1738 (2007)

**Key Words:** Peptide Self-Assembly, Empirical Force Fields, Molecular Dynamics, Replica Exchange Molecular Dynamics, Beta-Sheet, Beta-Barrel, Ring-Like Structure

**Send correspondence to:** Dr. Guanghong Wei, Department of Physics, Fudan University, Shanghai 200433, China, Tel: 86-21-55665231, Fax: 86-21-65104949, E-mail: ghwei@fudan.edu.cn

**http://www.bioscience.org/current/vol13.htm**